# Supporting information

# Highly ordered *n*/*p*-co-assembled materials with remarkable charge mobilities

*Javier López-Andarias,*[‡a] *María José Rodriguez,*[‡c] *Carmen Atienza,*[‡a] *Juan Luis López,*[a] *Tsubasa Mikie,*[d]

*Santiago Casado,*[b] *Shu Seki,*[c] *José L. Carrascosa*[b,c]**and Nazario Martín*[a,b]**

[a]Departamento de Química Orgánica I, Facultad de Ciencias Química, Universidad Complutense, E-28040 Madrid, Spain.

[b]IMDEA- Nanoscience, Campus de Cantoblanco, E-28049 Madrid, Spain.

[c]Centro Nacional Biotecnología (CNB)-CSIC, Spain.

[d]Department of Applied Chemistry, Graduate School of Engineering, Osaka University, 2-1 Yamadaoka, Suita, Osaka 565-0871, Japan.

**Contents:**


*1. Materials and Methods* *S3-S9*

*2. Supplementary Figures* *S10-S19*

*Absorption spectra of **2a** and **2b** in methanol* *S10*

*AFM images of **2a** and **2b*** *S10*

*Absorption spectra of **1**, **2b** and **$1_2$2b*** *S11*

*Absorption spectra of co-assembled **$1_2$2a** and **$1_2$2b*** *S11*

*CD spectra of co-assembled **$1_2$2a** and **$1_2$2b*** *S11*

*XPS spectra of co-assembled **$1_2$2a** and **$1_2$2b*** *S12*

*FTIR spectra of **1**, **2a**, **2b** and **$1_2$2a**, **$1_2$2b*** *S13*

*Photograph of the preparation of the closed sacs for SEM* *S13*

*SEM images of **$1_2$2a** and **$1_2$2b*** *S14*

*AFM images of **$1_2$2a** and **$1_2$2b*** *S14*

*TEM and HR-TEM images of **$1_2$2a** and **$1_2$2b*** *S15*

*Photographs from an optical microscope of **$1_2$2a** and **$1_2$2b*** *S16*

*Fluorescence confocal micrographs of **$1_2$2a** and **$1_2$2b*** *S16*

*XRD for **1**, **2a** and **2b*** *S17*

*Photo-conductivity transients observed for**$1_2$2a**, **$1_2$2b**, **1**, **2a** and **2b*** *S18*

*Anisotropic conductivity transients observed for **$1_2$2a**, **$1_2$2b*** *S18*

*Conductivity transients and TAS kinetic recorded for **$1_2$2a** and **$1_2$2b*** *S18*

*Anisotropic absorption of aligned film of **$1_2$2a**, **$1_2$2b*** *S19*

*3. References* *S20*

Reagents were purchased from Sigma-Aldrich, Acros or Fluka and were used without further purification. All solvents were dried by means of standard protocols with sodium and benzophenone as indicator. Column chromatography was carried out on silica gel 60 (Fluka, 40-63 $\mu$m). IR spectra were recorded on a Bruker Tensor 27 spectrometer equipped with ATR and reported as wavenumbers in $cm^{-1}$ with band intensities indicated as s (strong), m (medium), w (weak), br (broad). $^{1}H$ and $^{13}C$ NMR spectra were recorded either on a Bruker Avance-300 or a Bruker Avance AMX-700 and reported as chemical shifts ($\delta$) in ppm relative to tetramethylsilane ($\delta$ = 0) at room temperature unless other temperature was indicated. Spin multiplicities are reported as a singlet (s), broad singlet (br s), doublet (d), triplet (t) and quartet (q) with proton-proton coupling constants (*J*) given in Hz, or multiplet (m). Matrix-assisted laser desorption ionization (MALDI) mass spectrometry (MS) was performed on a Bruker Ultraflex spectrometer using ditranol as matrix. Absorption spectra were recorded with a Varian Cary 50 and 5000 spectrophotometer and UV-3600 Shimadzu UV-vis-NIR Spectrophotometer. The anisotropic absorption spectroscopy was carried out with a JASCO V-570 spectrometer with a polarizer. CD measurements were carried out on a JASCO J-815 DC spectrometer. Fluorescence images were recorded on a Leica SP2 confocal microscope ($\lambda_{exc}$= 514nm).

**X-ray photoelectron spectroscopy (XPS)**: the analysis was obtained on a SPECS GmbH (PHOIBOS 150 9 MCD) spectrometer working in the constant analyzer energy mode and a non monochromatic aluminium X-ray source (1486.61 eV) powered at 200 W and a voltage of 12 eV. For recording both survey and high resolution spectra pass energies of 75 and 25 eV were applied. Survey data were acquired from kinetic energies of 1487 – 400 eV with 0.1 eV of energy step and 100 ms dwell time per point. The high resolution scans were registered around the significant emission lines with 0.1 eV steps and 100 ms dwell time per point. The spectrometer control and data handling were monitorized using SpecsLab Version 2.48 software. Binding energies were calibrated relatively to the C 1s peak at 284.6 eV and the atomic ratios were computed from experimental intensity rations.

**Transmission Electron Microscopy (TEM)**: TEM images were performed in a JEOL JEM 1011 electron microscope operated at 100 kV. Images were directly recorded using a GATAN Erlangshen ES 1000W camera attached to the microscope. In the case of HR-TEM, images were acquired in a JEOL JEM 3000F electron microscope operated at 300 kV.

**Scanning Electron Microscopy (SEM)**: SEM images were acquired using a JEOL JSM 6335F microscope working at 10 kV.

**Atomic Force Microscopy (AFM)**: AFM images were performed using a JPK NanoWizard II, coupled to a Nikon Eclipse Ti-U inverted fluorescence optical microscope. NT-MDT NSG01 silicon tips grown on silicon cantilevers having typical values of 5.1 N/m for the force constant, and 150 kHz for the resonant frequency, were employed in dynamic mode at standard ambient conditions.

**X-ray Diffraction (XRD)**: XRD was performed in a Panalytical X'Pert PRO diffractometer with Cu tube (lambda K$\alpha$=1.54187 Å) operated at 45 kV, 40 mA, Ni beta filter, programmable divergence and anti-scatter slits working in fixed mode, and fast linear detector (X'Celerator) working in scanning mode. Samples were deposited in a silicon zero background sampleholder and measured in reflection mode"

**Small Angle X-ray Scattering (SAXS)**: The equipment for SAXS is a modified Kratky camera, enhanced by Hecus-Braun. This device is installed on a PANalytical X-ray generator PW3830.

## Synthesis

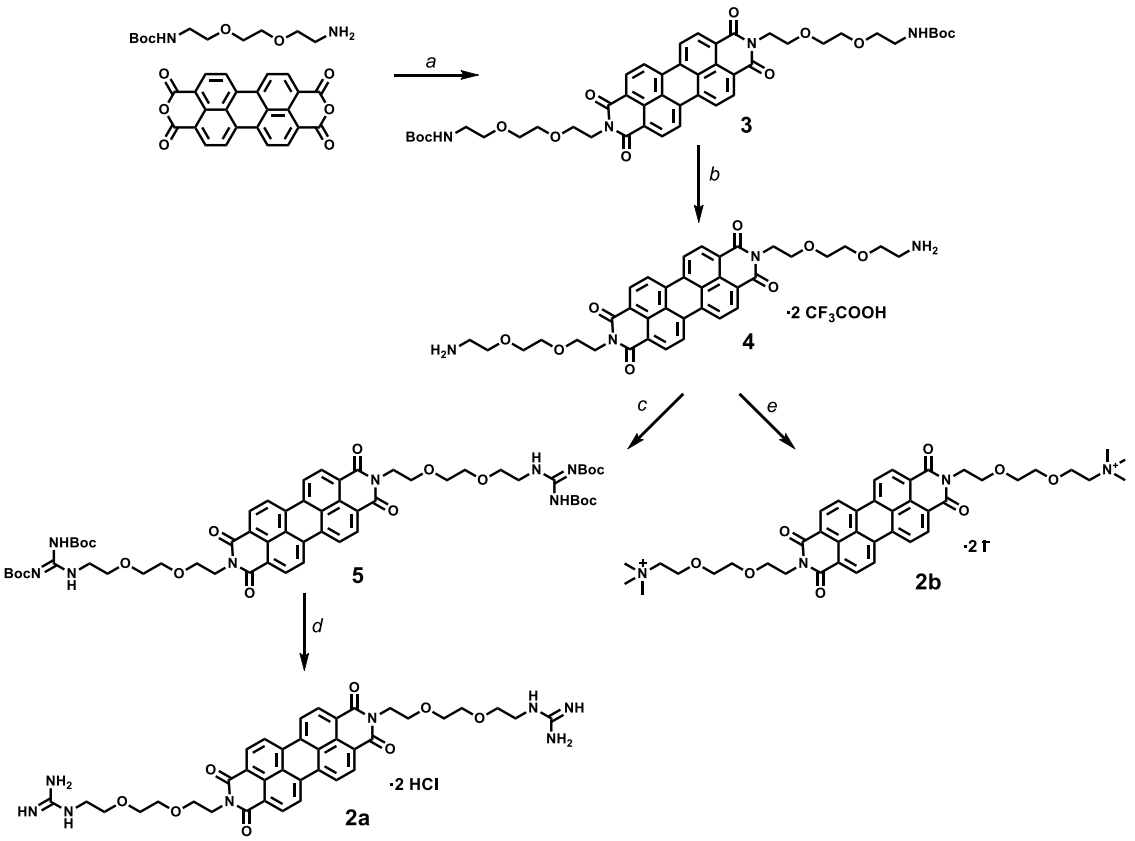


**Scheme S1.** a) $Zn(OAc)_2$, imidazole (80%); b) TFA / $CHCl_3$ (95%); c) 1,3-Bis(*tert*-butoxycarbonyl)-2-methyl-2-thiopseudourea, TEA, $HgCl_2$ / DMF (37%); d) HCl (*aq*) / MeOH (quant); e) $CH_3I$, $K_2CO_3$ / DCM:MeOH (62%).

**Compound 3.** N-Boc-2,2'-(ethylenedioxy)-diethylamine (1.3 g, 5.24 mmol), perylene-3,4,9,10-tetracarboxylic acid bisimide (690 mg, 1.75 mmol), zinc acetate (766 mg, 3.49 mmol) and imidazole (1 g) were stirred under argon atmosphere at 150 ºC for 3 hours. The reaction mixture was filtered through celite to remove the precipitate, and the filter was washed with $CH_2Cl_2$ (100 mL). After removing the solvent under reduced pressure, the crude product was purified by flash column chromatography ($SiO_2$, $CH_2Cl_2$/MeOH 30:1), to give **3** as a red solid (1.2 g, 80%). *Rf* = 0.19 (DCM:MeOH 20:1); IR: 2957 (m), 2926 (s), 2855 (m), 1695 (s), 1656 (s), 1594 (m), 1365 (m); $^1$H NMR (300 MHz, $CDCl_3$): 8.56 (d, 4H, $^3J$ (H,H) = 8.0 Hz), 8.40 (d, 4H, $^3J$ (H,H) = 8.0 Hz), 5.08 (br s, 2H), 4.51 (t, 4H, $^3J$ (H,H) = 5.8 Hz), 3.93 (t, 4H, $^3J$ (H,H) = 5.8 Hz), 3.81 - 3.74 (m, 4H), 3.69 - 3.62 (m, 4H), 3.55 (t, 4H, $^3J$ (H,H) = 5.2 Hz), 3.34 - 3.25 (m, 4H), 1.46 (s, 18H); $^{13}$C NMR (75 MHz, $CDCl_3$): 163.3, 156.0, 134.3, 131.2, 129.1, 126.1, 123.0, 123.1, 79.2, 77.3, 70.5, 70.3, 70.0, 68.0, 39.3, 28.5; MALDI ($[M+Na]^+$): calculated for $C_{46}H_{52}N_4O_{12}Na$: 875.35; found: 875.36.

**Compound 4.** A solution of **3** (1.0 g, 1.17 mmol) in $CHCl_3$ (6 mL) and TFA (4 mL) was stirred at room temperature for 1 h. The solvent was removed under reduced pressure. The solid residue was washed with $CHCl_3$ (25 mL) to remove any trace of starting material and then dried under vacuum. The pure compound was obtained as a red solid without further purification (830 mg, 95%). IR: 2959 (w),

2927 (m), 1694 (s), 1655 (s), 1594 (m), 1204 (m), 1129 (m); $^1$H NMR (300 MHz, $CD_3OD$): 8.02 (d, 4H, $^3J$ (H,H) = 8.0 Hz), 7.91 (d, 4H, $^3J$ (H,H) = 8.0 Hz), 4.33 (t, 4H, $^3J$ (H,H) = 6.0 Hz), 3.86 (t, 4H, $^3J$ (H,H) = 6.0 Hz), 3.83 - 3.78 (m, 4H), 3.78 - 3.70 (m, 8H), 3.16 (t, 4H, $^3J$ (H,H) = 5.2 Hz); $^{13}$C NMR (75 MHz, $CDCl_3$): 163.1, 133.4, 130.5, 128.0, 124.7, 123.5, 122.1, 70.4, 70.3, 67.9, 66.9, 39.7, 39.5; MALDI ($[M+H]^+$): calculated for $C_{36}H_{37}N_4O_8$: 653.26; found: 653.13.

**Compound 5.** To a solution of diamine **4** (500 mg, 0.57 mmol) in dry DMF (10 mL) were added 1,3-bis(*tert*-butoxycarbonyl)-2-methyl-2-thiopseudourea (330 mg, 1.14 mmol) and TEA (0.475 mL, 3.41 mmol). The mixture was stirred at room temperature for 5 min. To the resulting solution, $HgCl_2$ (340 mg, 1.25 mmol) was added and the mixture was allowed to react at room temperature. After 30 min, it was diluted with $CH_2Cl_2$ (100 mL) and filtered through celite to remove the precipitate, and the filter was washed with $CH_2Cl_2$ (100 mL). The filtrate was washed with a saturated $NH_4Cl$ aqueous solution (3 x 100 mL), water (2 x 100 mL) and brine (100 mL). The organic layer was dried over $Na_2SO_4$ and the solvent was removed under reduced pressure. The crude product was purified by flash column chromatography ($SiO_2$, $CH_2Cl_2$/MeOH 30:1) affording **6** as a red solid (240 mg, 37%). *Rf* = 0.26 (DCM:MeOH 20:1); IR: 3328 (br), 2956 (m), 2924 (s), 285 (m), 1698 (s), 1645 (s), 1367 (m), 1140 (s);$^1$H NMR (300 MHz, $CDCl_3$): 11.42 (s, 2H), 8.79 (br s, 2H), 8.32 (d, 4H, $^3J$ (H,H) = 8.0 Hz), 8.09 (d, 4H, $^3J$ (H,H) = 8.0 Hz), 4.49 (t, 4H, $^3J$ (H,H) = 5.2 Hz), 3.95 (t, 4H, $^3J$ (H,H) = 5.2 Hz), 3.86 - 3.64 (m, 16H), 1.57 (s, 18H), 1.49 (s, 18H); $^{13}$C NMR (75 MHz, $CDCl_3$): 163.3 156.7, 153.0, 136.9, 133.9, 131.2, 128.8, 123.1, 122.8, 83.8, 77.4, 70.4, 69.9, 69.6, 68.3, 41.1, 39.7, 28.4, 28.2; MALDI ($[M+Na]^+$): calculated for $C_{58}H_{72}N_8O_{16}Na$: 1159.50; found: 1159.50.

**Compound 2a.** To a solution of **5** (150 mg, 0.13 mmol) in MeOH (5 mL), HCl (*aq*) (2 mL) was added and the mixture was stirred at room temperature. After 20 h, the solvent was removed under reduced pressure. The solid residue was precipitated and centrifuged in cold diethyl ether to remove any trace of impurities and then dried under vacuum. The pure compound was obtained as a purple solid without further purification (105 mg, 99%). IR: 3316 (br), 3173 (br), 1694 (m), 1654 (s), 1594 (m), 1344 (w); $^1$H NMR (700 MHz, DMSO-$d_6$, 50 ºC): 8.54 (d, 4H, $^3J$ (H,H) = 6.5 Hz), 8.31 (d, 4H, $^3J$ (H,H) = 6.5 Hz), 7.53 (t, 2H, $^3J$ (H,H) = 4.7 Hz), 7.12 (br s, 8H), 4.26 (t, 4H, $^3J$ (H,H) = 5.8 Hz), 3.73 (t, 4H, $^3J$ (H,H) = 5.8 Hz), 3.65 (t, 4H, $^3J$ (H,H) = 4.5 Hz), 3.59 (t, 4H, $^3J$ (H,H) = 4.5 Hz), 3.51 (m, 4H, $^3J$ (H,H) = 4.8 Hz), 3.29 – 3.26 (m, 4H); $^{13}$C NMR (175 MHz, DMSO-$d_6$, 50 ºC): 163.0, 157.7, 134.1, 131.1, 128.6, 125.6, 124.4, 122.7, 70.2, 70.1, 69.1, 67.5, 41.4, 39.4; HR-MALDI ($[M+H]^+$): calculated for $C_{38}H_{41}N_8O_8$: 737.3047; found: 737.3042.

**Compound 2b.** To a solution of **4** (60 mg, 0.068 mmol) and $K_2CO_3$ (190 mg, 1.37 mmol) in $CH_2Cl_2$:MeOH (5 mL, 3:1 v:v), was added iodomethane (36$\mu$L, 0.58 mmol) and the reaction mixture was allowed to react at room temperature for 24 hours. The solid residue was isolated by filtration through celite followed by rotary evaporation. The product was precipitated and centrifuged in cold diethyl ether to remove any trace of impurities and then dried under vacuum. The pure compound was obtained as a purple solid without further purification (42 mg, 62%). IR: 3348 (br), 1636 (s), 1451 (w), 1316 (m), 1084 (w); $^1$H NMR (700 MHz, DMSO, 50 ºC): 8.84 (d, $^3J$ (H,H) = 8.2 Hz, 4H), 8.51 (d, $^3J$ (H,H) = 8.2 Hz, 4H), 4.29 (t, $^3J$ (H,H) = 6.5 Hz, 4H), 3.88 – 3.84 (m, 4H), 3.75 (t, $^3J$ (H,H) = 6.5 Hz, 4H), 3.65 (dd, $^3J$ (H,H) = 5.6, 3.0 Hz, 4H), 3.62 (dd, $^3J$ (H,H) = 5.6, 3.0 Hz, 4H), 3.60 – 3.56 (m, 4H), 3.15 (s, 18H);$^{13}$C NMR (175 MHz, DMSO, 50 ºC): 163.2, 134.5, 131.5, 128.9, 126.0, 124.7, 123.0, 69.9, 69.9, 67.6, 65.0, 64.6, 53.7, 39.5; HR-MALDI ($[M]^+$): calculated for $C_{42}H_{50}N_4O_8$: 738.3629; found: 738.3630.

## $^{1}$H NMR and $^{13}$C NMR of Compound 2a

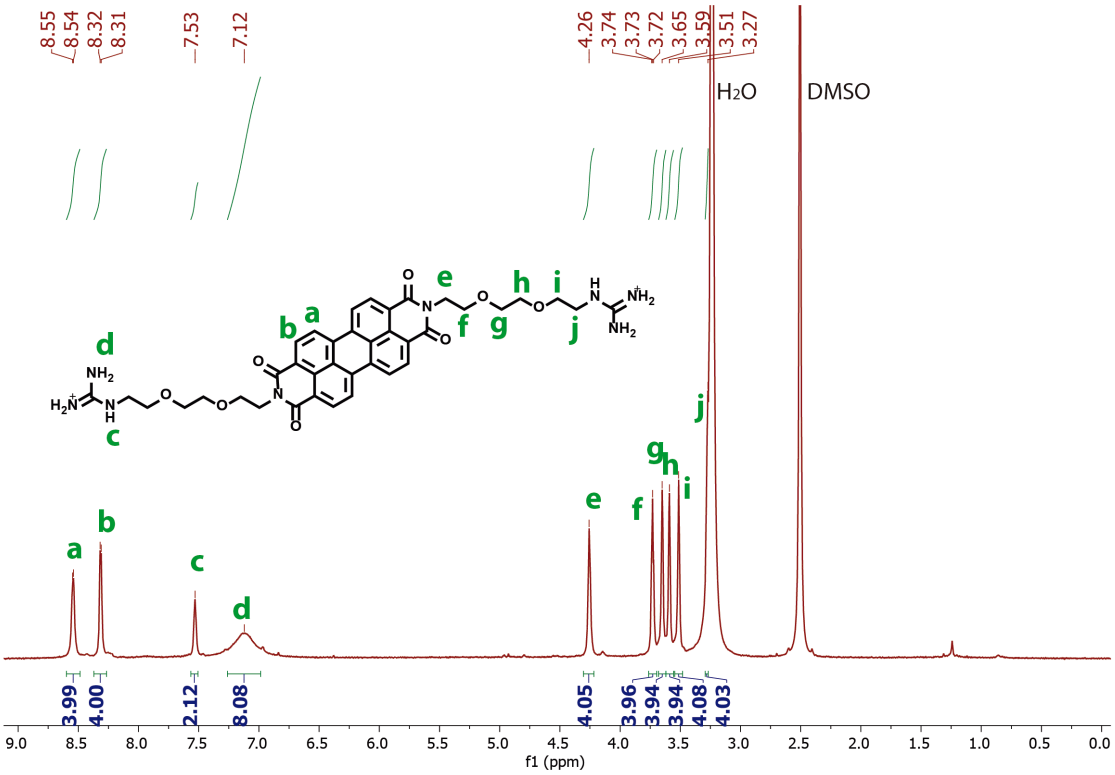


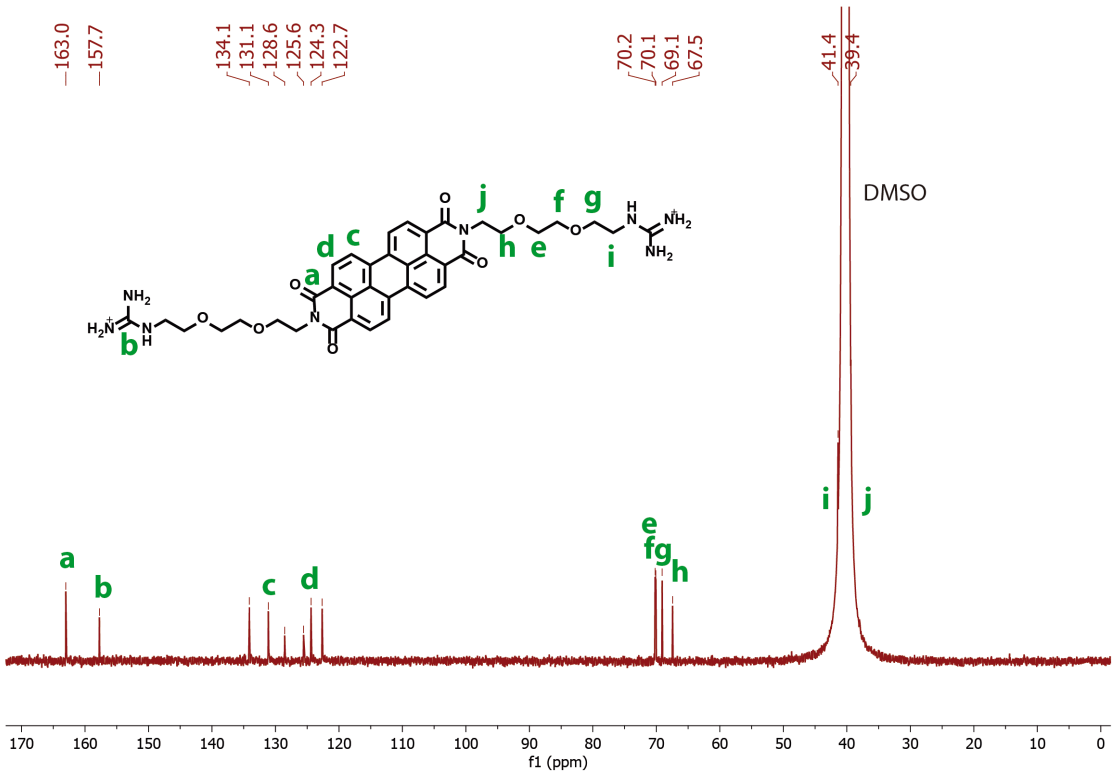

**$^{1}$H NMR and $^{13}$C NMR of Compound 2b**

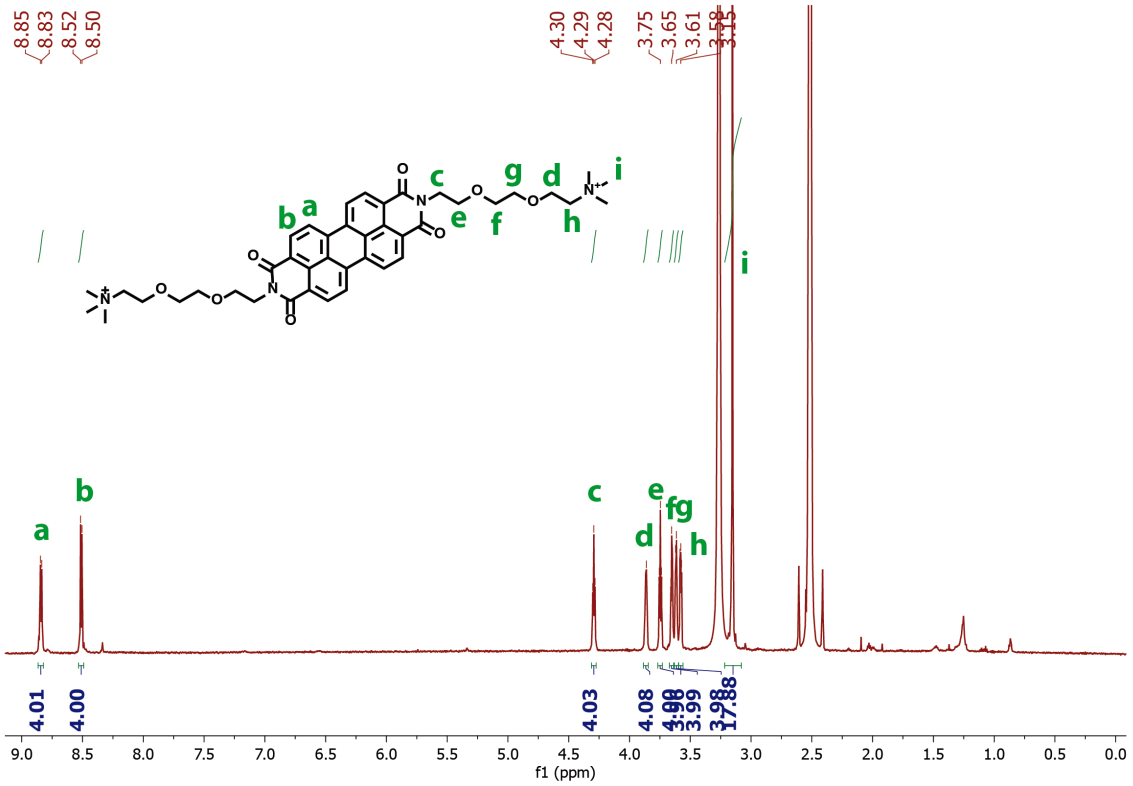


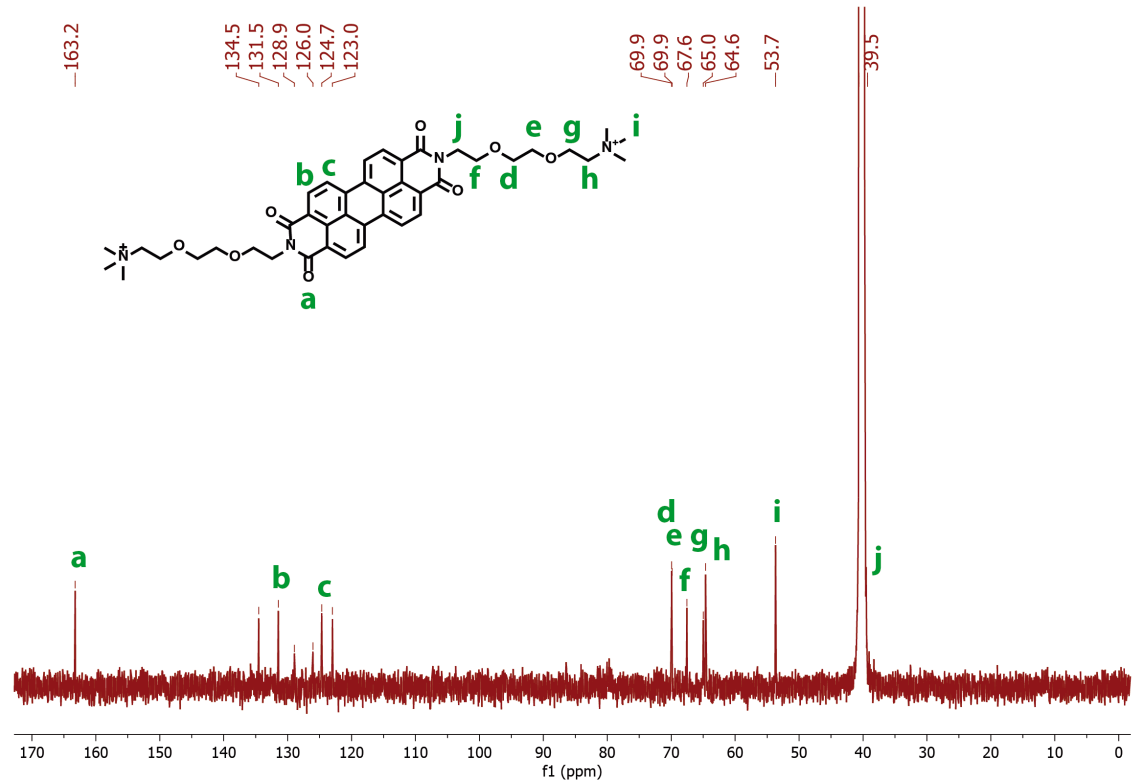

**FP-TRMC and TAS measurements.**

Nanosecond laser pulses from a Nd:YAG laser of Spectra-Physics INDI-HG(full width at half maximum ($\phi\Sigma\mu$) of 5－8 ns) was used as an excitation light sourse, and the third harmonic generation (THG)(355 nm) were exposed to the solid films of **1**, **2a**, **2b**, **1**$_2$**2a**, and **1**$_2$**2b**. The laser power density was set to 5.1 mJ/cm$^2$ (9.1 × 10$^{15}$ photons/cm$^2$). For TRMC measurements, the microwave frequency and power were set at approximately 9.1 GHz and 3mW, respectively, and the TRMC signal was evoluted in a diode (rise time < 1 ns), and output signal was led into a digital oscilloscope of Tektronix TDS 3032B. All experiments described above were conducted at room temperature. Reflected power change ratio ($\Delta P_r/P_r$) of microwave from the cavity in FP-TRMC apparatus is in relation with the total loss ($\Delta(1/Q)$) of microwave by the photo-induced transient species in the cavity as follows[1]:

$$\frac{\Delta P_r}{P_r} = \frac{\left(\frac{1}{Q}\right)}{\left(\frac{\Delta\omega}{\omega_0}\right)^2 + \left(\frac{1}{2Q}\right)^2} \Delta\left(\frac{1}{Q}\right) \quad (1),$$

where, $\omega_0$ and $\Delta\omega$ are the resonant frequency of 9.1 GHz and its shift by the photo-induced transient species. The loss and the frequency shift of the microwave are expressed as a function of complex conductivity ($\Delta\sigma_r + i\Delta\sigma_i$) of the transient species by:

$$\Delta\left(\frac{1}{Q}\right) - i\frac{2\Delta\omega}{\omega_0} = F\left(\Delta\sigma_r + i\Delta\sigma_i\right) \quad (2),$$

where $F$ is a calibration factor derived from the measurements of total loss of microwave in the cavity loaded with materials with well-known conductivity values. The value of $\Delta P_r/P_r$ will be proportional to the sum of the mobilities ($\Sigma\mu$) of charged species in case of negligibly small $\Delta\omega$:

$$\Delta\sigma_r = N\phi\sum\mu = A\frac{\Delta P_R}{P_R} \quad (3),$$

where $N$, $\phi$, and A are the number of absorbed photons, photo-carrier separation quantum yield, and a sensitivity factor (constant), respectively. Details in the sensitivity factor, A are described elsewhere.[2]

To determine the values of $\phi$, we conducted transient optical absorption spectroscopy at 25 °C using solid film of deposited onto an identical quartz substrate to that in FP-TRMC measurements.[3] Transimittance of excitation light pulses was measured by a PE25 power meter of Ophir Optoronics Ltd., leading to the > 99% absorbance of the films for the laser pulses. Time-dependent absorption spectral changes were monitored by Hamamatsu C7700 streak camera via a Hamamatsu C5094 spectrometer upon excitation of the film with 355 nm light pulses from an identical laser system for TRMC measurements. The excitation density was tuned at 5.5 × 10$^{16}$ cm$^{-2}$ photons per pulse. The streak scope images were averaged over 1600 images to correct a 2-dimensional time-wavelength correlation data of the transient absorption. The values of f were calculated on the assumption of balanced charges of holes and electrons on **1** and **2a** or **2b**, respectively. On the basis of the molar extinction coefficients of PBI radical anions ($\varepsilon^-$ = 7.4 × 10$^4$ mol$^{-1}$dm$^3$cm$^{-1}$), the values of $\phi$ was determined as 2.2 and 2.8 × 10$^{-4}$, respectively in **1**$_2$**2a** and **1**$_2$**2b** systems.

**Decay analysis.**

The charge recombination of the positive and negative charger via isotropic diffusion in the crystal obeys second-order reaction expressed by the next expression of a form:

$$\frac{1}{N(t)} = k\ t + 1/N(0) \qquad (4)$$

where $k_1$ denote the second-order rate constant, and $N$(t) is proportional to the conductivity transients. According to eq. (4), the apparent values of $k$ are estimated as 5.5, 3.0, and 0.8 μs, respectively for **$1_2$2a**, **$1_2$2b**, and **1** by the fitting of the reciprocal kinetic traces in figure S16.

**General method for the preparation of $1_2$2a and $1_2$2b *n*/*p*-co-assembled nanostructures**

*Randomly distributed fibers for UV, CD and XPS spectroscopy, TEM and AFM imaging:* In a typical experiment, around 0.75 mL of 5 x $10^{-3}$ M aqueous solution of **1** in the presence of 7.5 eq of $NaHCO_3$ is mixed with around 0.75 mL of 5 x $10^{-3}$ M aqueous solution of **2a** or **2b**, obtaining an homogeneous reddish powder within the solution. This powder was centrifuged at high rpm rate (1 x $10^4$ rpm for 5 min) in an Eppendorf microcentrifuge tube to clean from the excess of starting materials. The upper 75% of the supernatant was removed from the centrifugation tubes and around 1 mL of cleaned deionized water was added. The Eppendorf tube was shacked until an homogeneous dispersion was obtained and it was centrifuged again. This process was repeated until obtaining a colourless supernatant. In the case of XPS analysis, the samples were introduced in the apparatus as powder coated over a polycarbonate membrane. In the case of TEM studies, samples were negatively stained with 2% uranyl acetate on carbon coated grids for 1 minute as follows: A small drop of the sample is deposited on the carbon coated grid, allowed to settle/incubate for approximately one minute, blotted dry, washed with water for 5 minutes and then covered with a small drop of the stain (2% uranyl acetate). After 1 minute, this drop was also blotted dry and washed with water. In the case of AFM, samples were drop-casted on #2 Menzel-Gläser Ø 24 mm cover slides.

*Closed sacs with aligned fibers in the membrane, for SEM imaging:* These sacs were made by injecting one drop of a concentrated aqueous solution of one of **1** or **2a**/**2b** (5 x $10^{-3}$ M), directly into the bulk of the other, **2a**/**2b** or **1** (5 x $10^{-3}$ M), respectively (Figure S7). After 2-3 days, the liquid phase was carefully removed and the closed sac was fixed by an aqueous solution of glutaraldehyde and paraformaldehyde (2.5% and 4% respectively) for two hours. After washing several times with deionized water, sample dehydration was carried out by slow exchanging with a gradient of water-ethanol mixtures (30, 50, 70 up to 100% of ethanol) until the sac was in 100% ethanol. Samples were inmersed in each solution for at least 10 min. The ethanol was removed by critical point drying (CPD) to preserve the structure of the sample for SEM analysis. Dried sacs were deposited on graphite and were metalized with Au before observation.

*Aligned bundled filaments, for optical and fluorescence confocal microscopy:* These macroscopic filaments were made by slowly injecting **1** or **2a**/**2b** (5 x $10^{-3}$ M) with a needle of 0.8 mm diameter into the bulk of the other, **2a**/**2b** or **1** (5 x $10^{-3}$ M), respectively. After some minutes, these filaments were directly taken out of the solution using fine tweezers and deposited onto a glass slide without further treatment.

## Supporting Figures

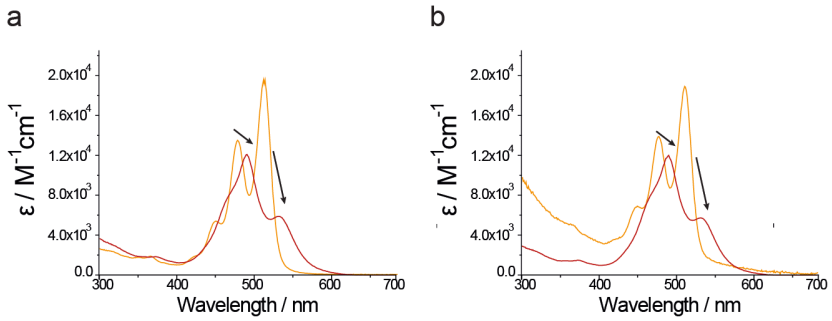


**Figure S1.** Absorption spectra of **2a** (a) and **2b** (b) in methanol (orange) and water (purple). Arrows show changes in the absorption maxima.

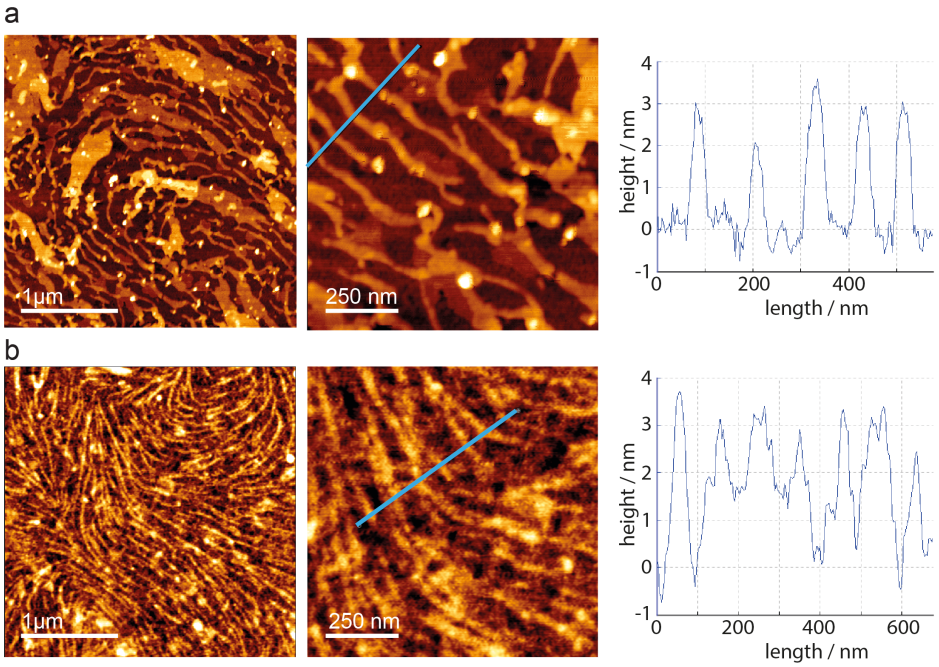


**Figure S2.** AFM images of **2a** (a) and **2b** (b) deposited onto a cover slide, from aqueous solution (MilliQ water, 5 x $10^{-5}$ M).

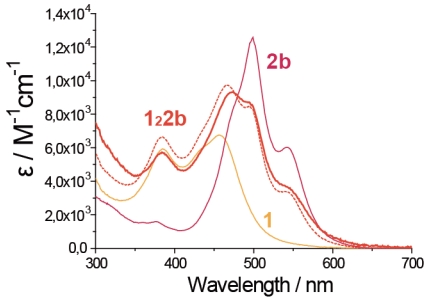


**Figure S3.** Absorption spectra for aqueous solutions of **1** (yellow), **2b** (purple) and for the dispersion obtained by mixing of both solutions (solid orange). Dashed orange line represents the simulated spectra for mixture with a stoichiometry of $\mathbf{1}_2\mathbf{2b}$.

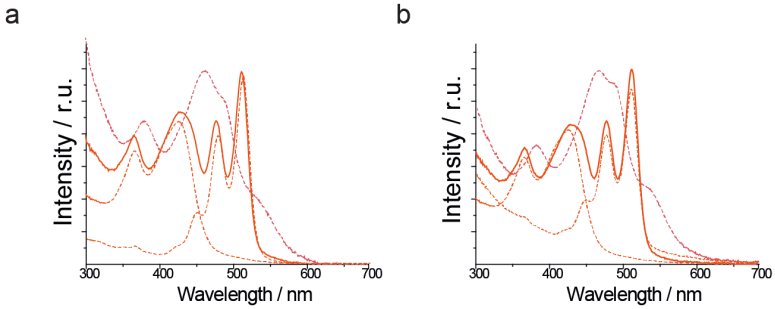


**Figure S4.** Absorption spectra of co-assembled $\mathbf{1}_2\mathbf{2a}$ (a) and $\mathbf{1}_2\mathbf{2b}$ (b) before addition of a protic polar solvent (dash purple line), and after the addition (solid orange line) to probe the reversibility of the supramolecular interactions. Dash orange lines correspond to isolated molecules **1**, **2a** and **2b** in methanol.

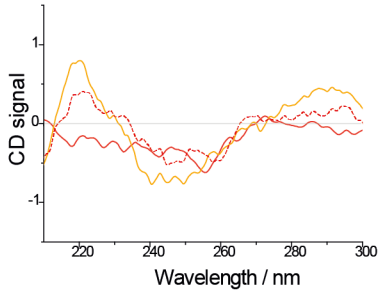


**Figure S5.** Circular dichroism spectral changes for aqueous solution of **1** upon addition of **2b** in the chromophores absorption range. Circular dichroic spectra in the peptide absorption range of **1** (orange), $\mathbf{1}_2\mathbf{2a}$ (red solid) and $\mathbf{1}_2\mathbf{2b}$ (red dashed) demonstrating the permanence of the β-sheet secondary structure within the n/p-co-assembled nanostructure.

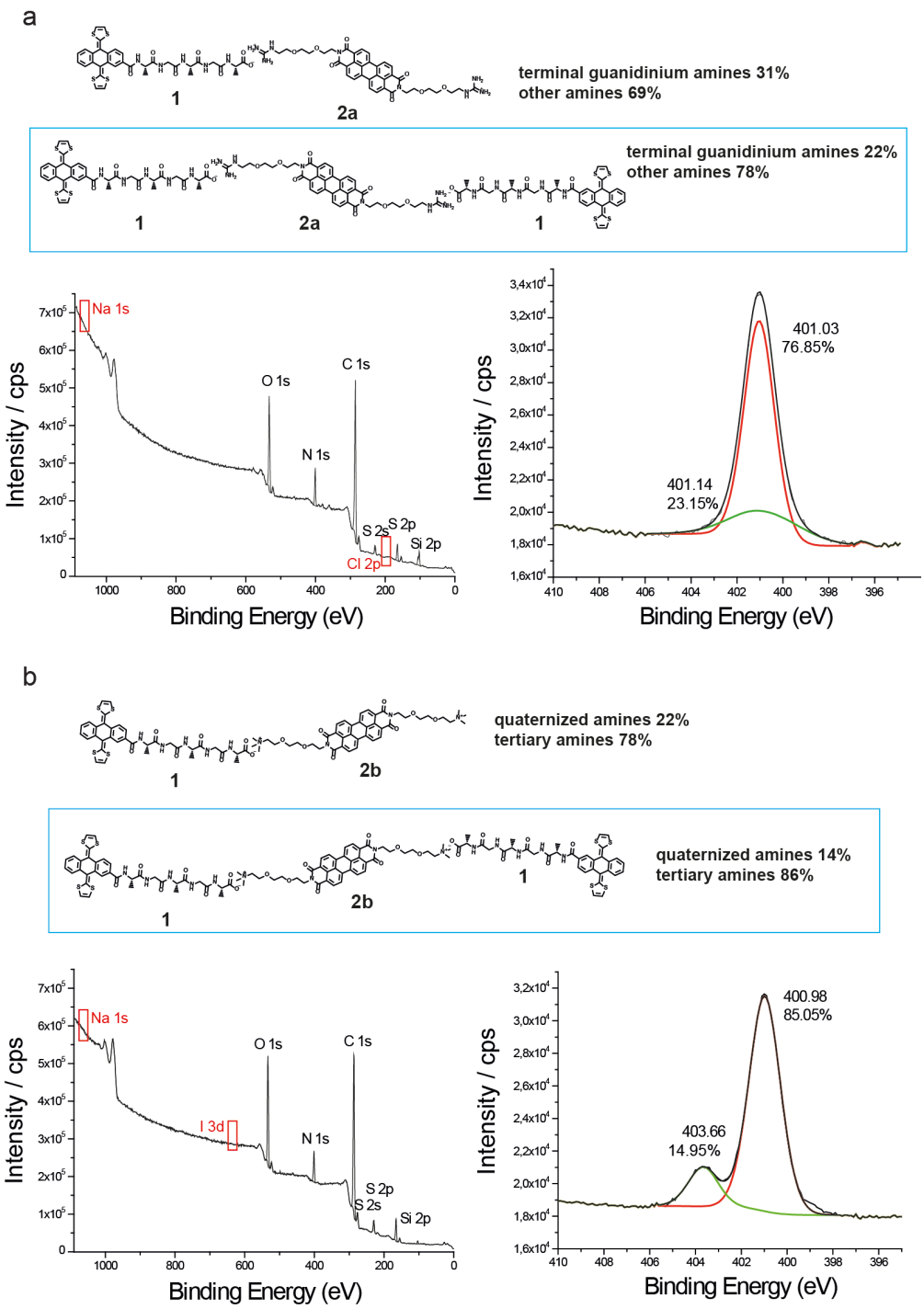


**Figure S6.** XPS survey spectra of a solid sample $\mathbf{1}_2\mathbf{2a}$ (a) and $\mathbf{1}_2\mathbf{2b}$ (b). (Left) Full spectrum; (Right) High-resolution XPS spectrum of the N-1s region; Gaussian deconvolution of the N-1s signal determines the populations of electronically distinct N atoms. Note that this deconvolution demonstrates the quantitative ionic interactions between exTTFs and PBIs at the molecular level, that is, two molecules of exTTF (one carboxylate group each) per one molecule of PBI (two guanidinium or ammonium groups each). This experimental data is more obvious in the case of $\mathbf{1}_2\mathbf{2b}$, where the difference between the binding energy of the cationic amines and the rest of amines is bigger, resulting in a more accurate deconvolution of the N-1s signal.

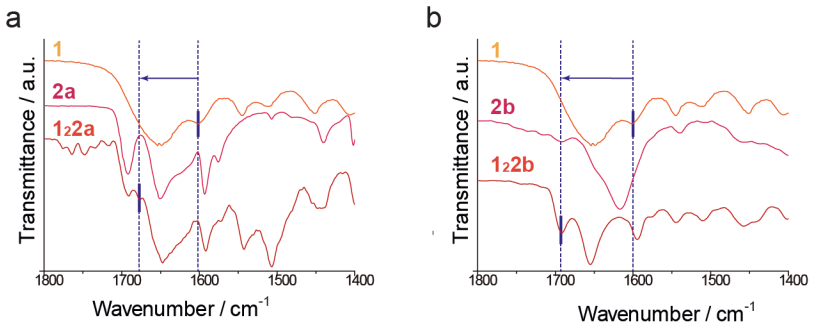


**Figure S7.** FTIR spectra of **1**, **2a** and **1$_2$2a** (left) and **1**, **2b** and **1$_2$2b** (right) showing the shift on the carboxylate band of compound **1** when forming the *n*/*p*-co-assembled material.

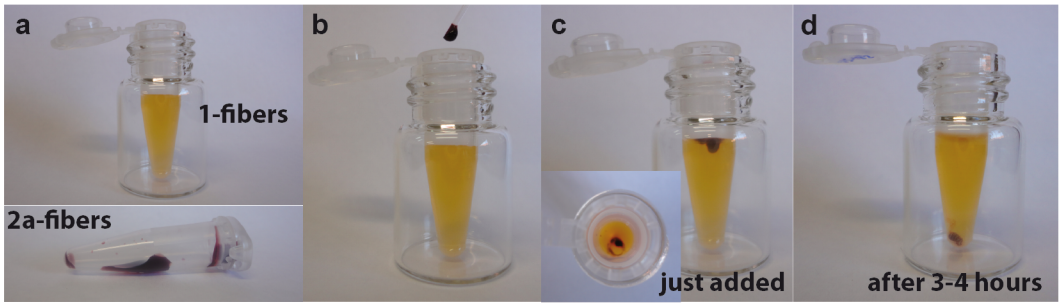


**Figure S8.** Procedure for the preparation of closed sacs, for SEM imaging of aligned fibers in the liquid-liquid interface between both self-assembled molecules. In this example, one drop of **2a** is added into the bulk of a solution of **1**. This methodology can be carried out also for **2b** and in the opposite sense, as well.

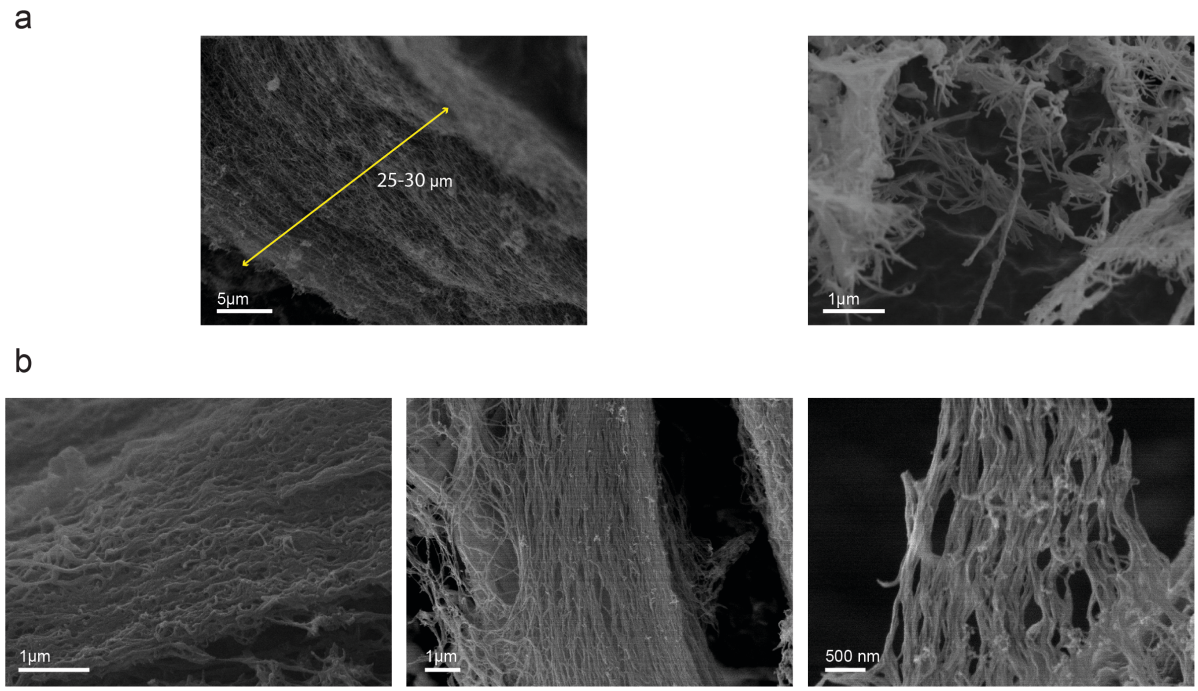


**Figure S9.** SEM images of **$1_2$2a** (a) and **$1_2$2b** (b) dehydrated samples.

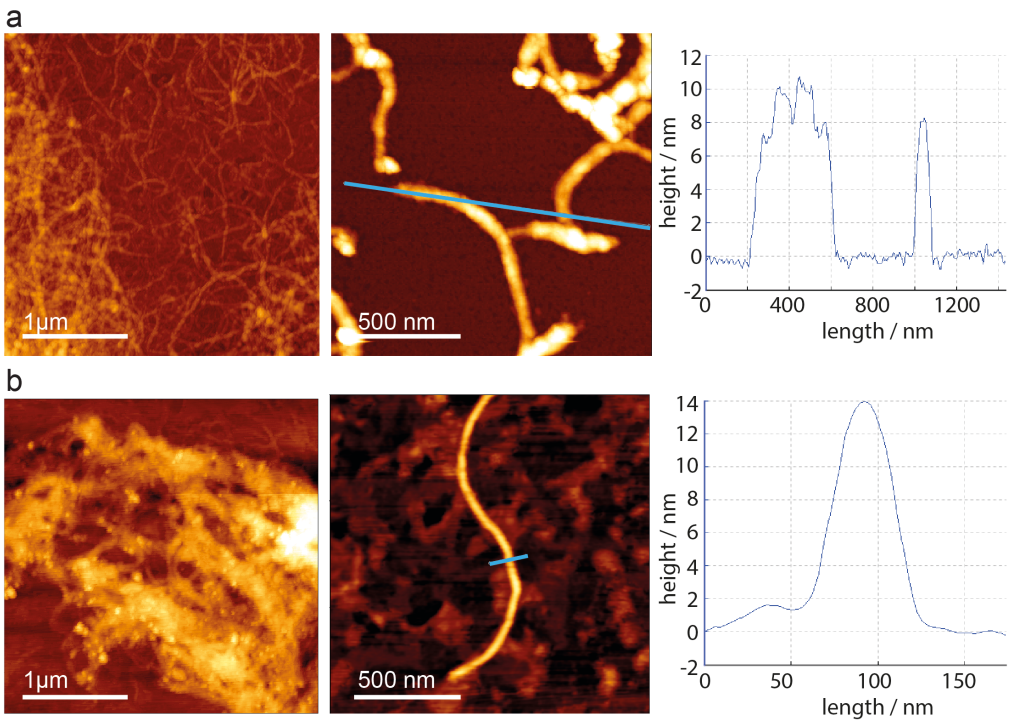


**Figure S10.** (Left and centre) AFM images at different length scales of randomly distributed fibers of **$1_2$2a** (a) and **$1_2$2b** (b) n/p-co-assembled nanostructures. (Right) Height profile across the blue line.

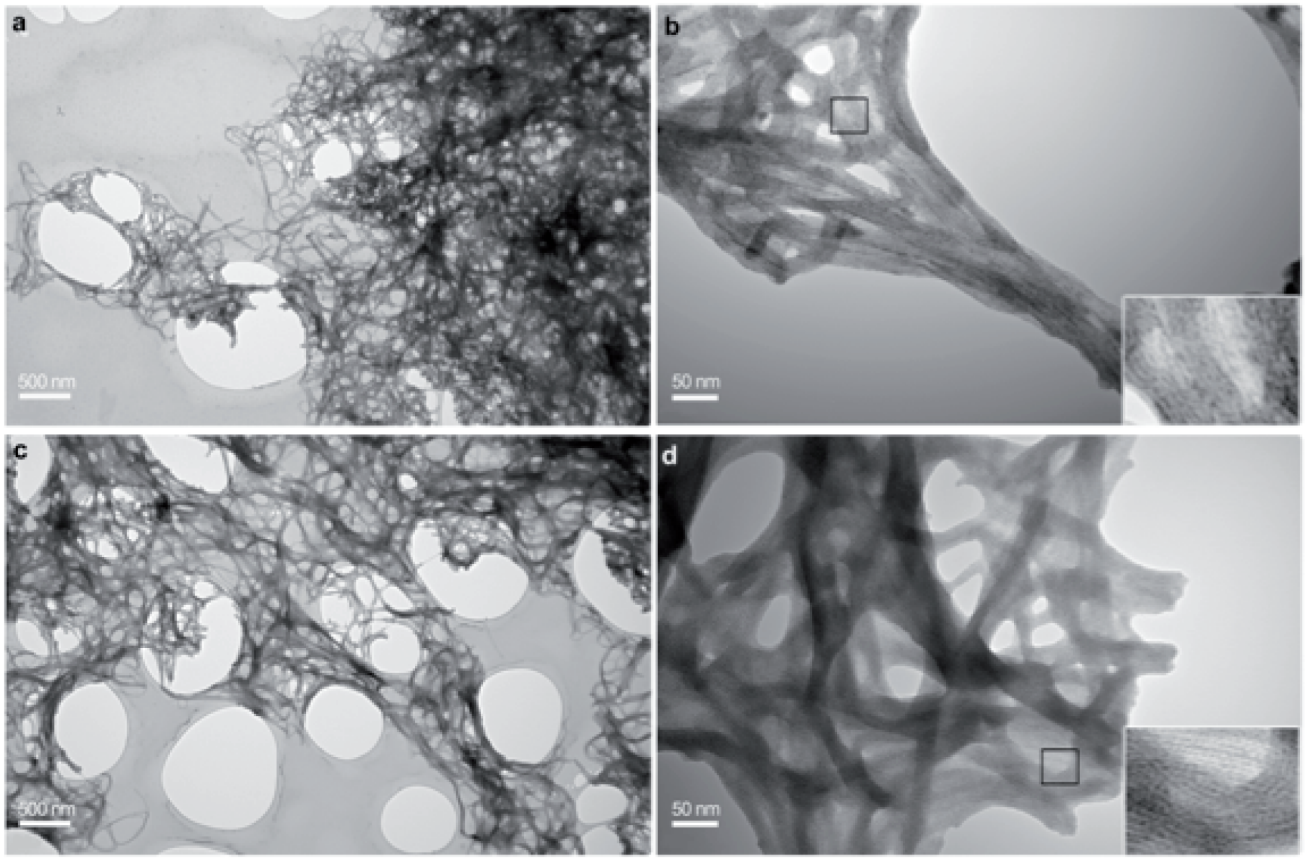


**Figure S11.** TEM images at different length scales of randomly distributed fibers of $\mathbf{1_2}$**2a** (a,b) and $\mathbf{1_2}$**2b** (c,d) n/p-co-assembled nanostructures.

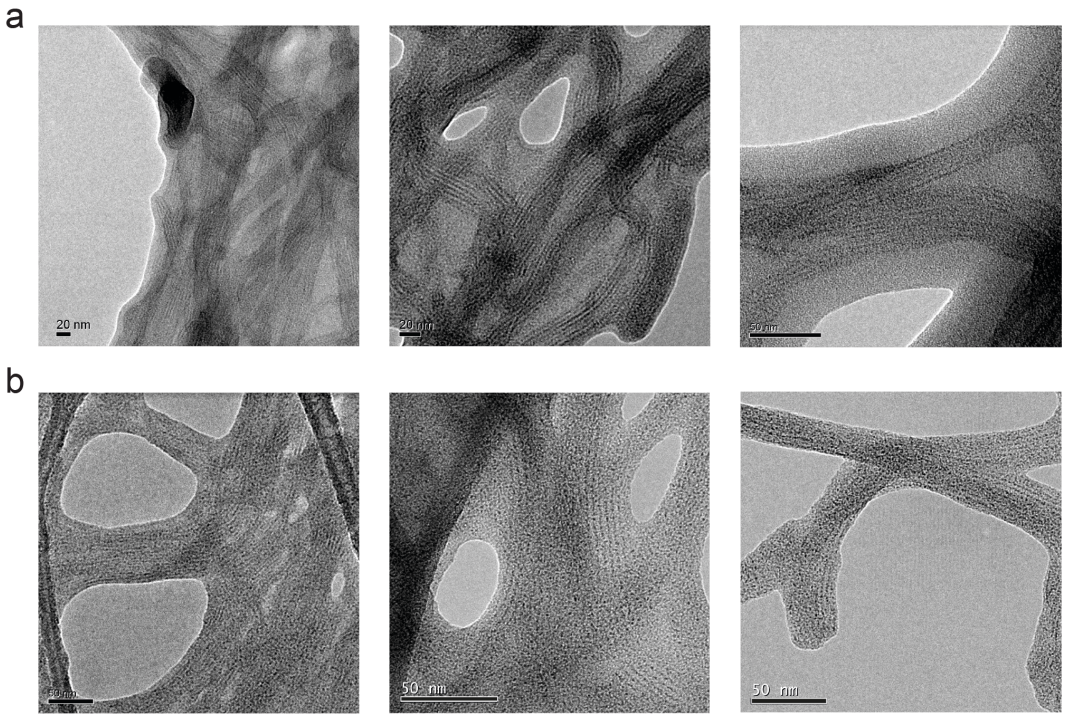


**Figure S12.** HR-TEM images of randomly distributed fibers of $\mathbf{1_2}$**2a** (a) and $\mathbf{1_2}$**2b** (b) n/p-co-assembled nanostructures.

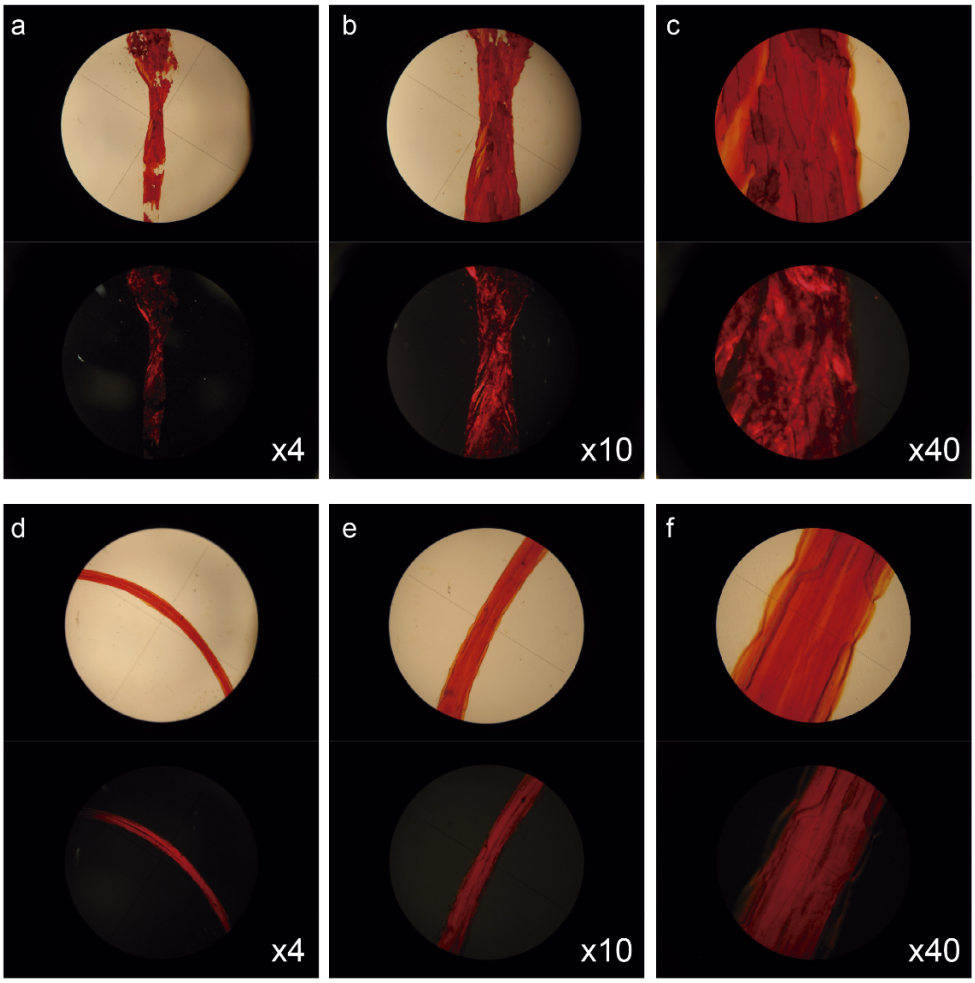


**Figure S13.** Photographs from an optical microscope of macroscopically aligned bundled filaments of $\mathbf{1}_2$**2a** (a-c) and $\mathbf{1}_2$**2b** (d-f), at different amplifications, using non-polarized (top) and polarized light (bottom).

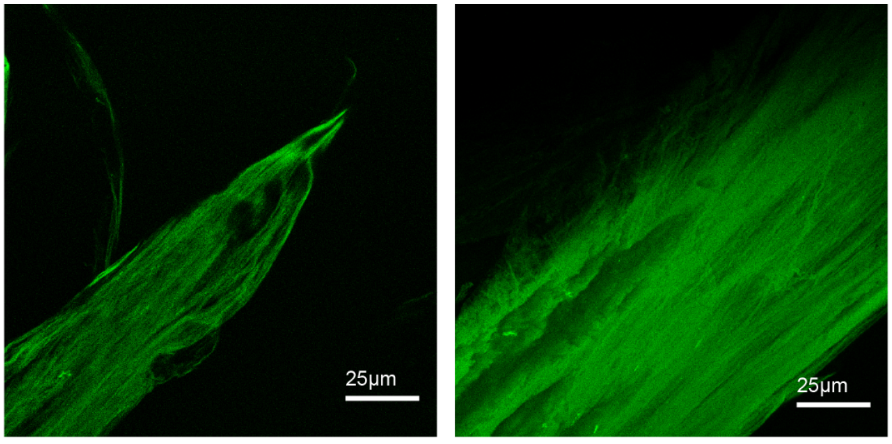


**Figure S14.** Fluorescence confocal micrographs of different regions of a filament obtained from $\mathbf{1}_2$**2b** *n*/*p*-co-assembled nanostructure.

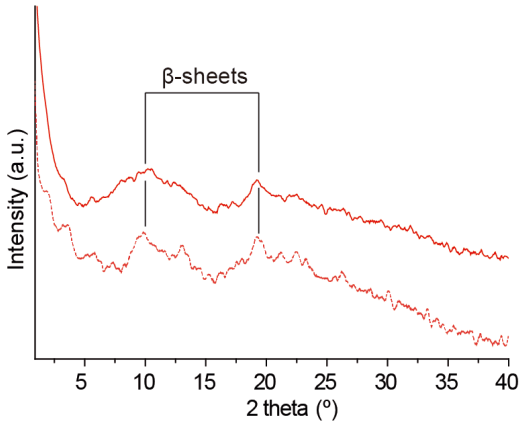


**Figure S15**. XRD patterns of *n*/*p*-co-assembled **1**$_2$**2a** (solid red) and **1**$_2$**2b** (dashed red).

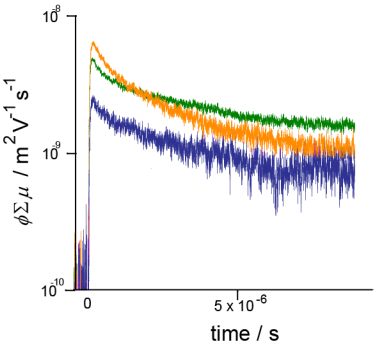


**Figure S16**. Photo-conductivity transients observed for **1**(orange), **2a** (green) and **2b** (blue), respectively**.** The excitation was carried out at 355 nm, 9.1×10$^{15}$ photons/cm$^2$.

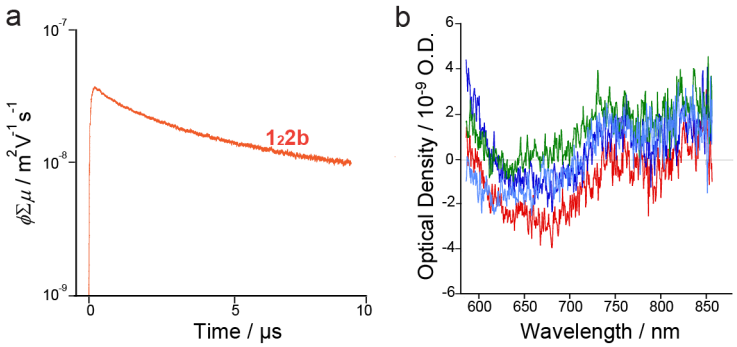


**Figure S17**. (a) Conductivity transients observed for **1**$_2$**2b** upon exposure for 355 nm, 9.1 ×10$^{15}$ photons/cm$^2$. (b) Transient absorption spectra recorded for **1**$_2$**2b** in solid films, upon excitation at 355 nm, 5.5 ×10$^{16}$ photons/cm$^2$. The red, green, and blue spectra were recorded immediately after the pulse exposure of **1** (red), **2** (green), and **8** (blue) $\mu$s, respectively.

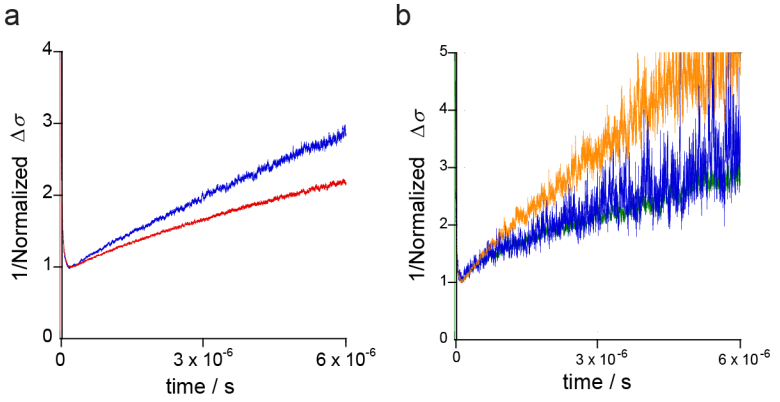


**Figure S18**. Reciprocal normalized photo-conductivity transients observed for (a) $\mathbf{1}_2$**2a** (red) and $\mathbf{1}_2$**2b** (blue), (b) **1** (orange), **2a** (green) and **2b** (blue), respectively**.** The excitation was carried out at 355 nm, $9.1\times10^{15}$ photons/cm$^2$.

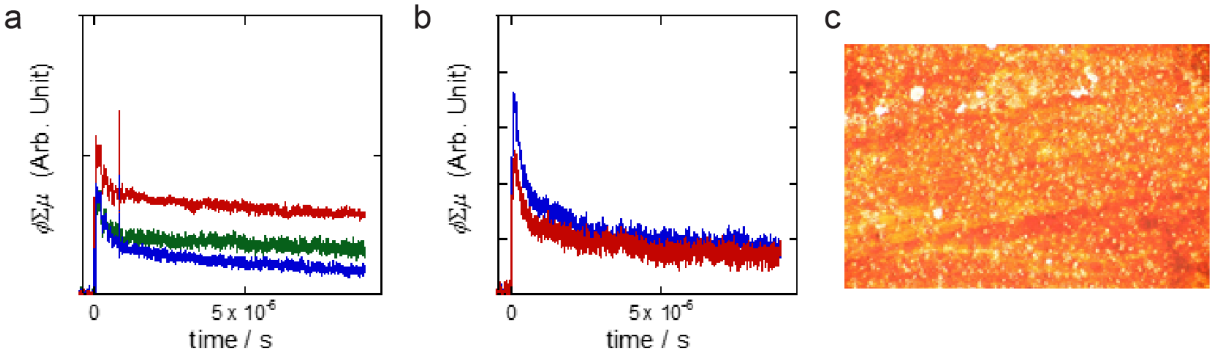


**Figure S19**. Anisotropic conductivity transients observed for (a) $\mathbf{1}_2$**2a** and (b) $\mathbf{1}_2$**2b** deposited on a quartz substrate under controlled orientation by rubbing. Blue and red transients were observed along the directions rectangular and parallel to the rubbing direction. All transients were observed upon excitation to 355 nm, $9.1\times10^{15}$ photons/cm$^2$. The kinetic trace was also observed for an identical oriented sample of $\mathbf{1}_2$**2a** nanofibres under Ar (blue) and $SF_6$ (green) atmospheres. (c) Optical microscope image of the rubbed film of $\mathbf{1}_2$**2a**.

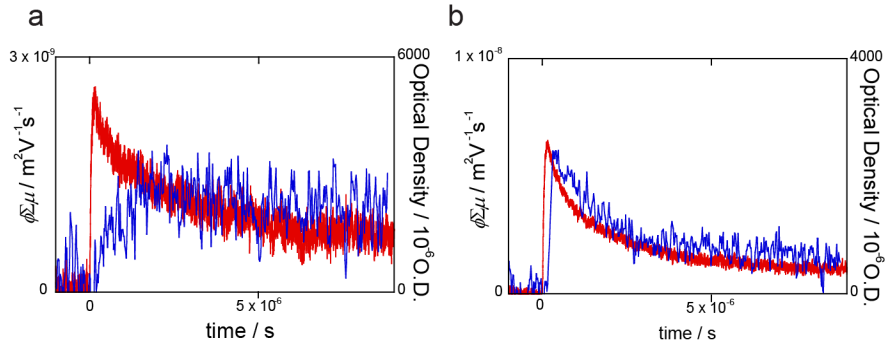


**Figure S20.** Conductivity transients and TAS kinetic traces at 740 – 750 nm recorded for (a) $\mathbf{1}_2$**2a** and (b) $\mathbf{1}_2$**2b** solid films, respectively upon excitation at 355 nm, $5.5\times10^{16}$ photonscm$^{-2}$. Red and blue transients were TRMC and TAS kinetic traces, respectively.

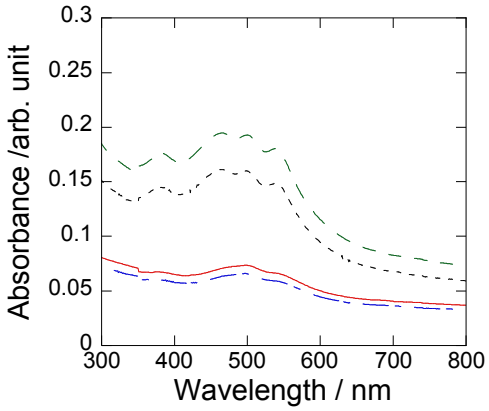


**Figure S21.** Anisotropic absorption of aligned film of $\mathbf{1}_2\mathbf{2a}$ (black and green) and $\mathbf{1}_2\mathbf{2b}$ (red and blue) by rubbing.

## REFERENCES


[1] Slater, J. C. *Rev. Mod. Phys.* **18** (1946) 441-512

[2] a) F. C. Grozema, L. D. A. Siebbeles, J. M. Warman, S. Seki, S. Tagawa, U. Scherf, *Adv. Mater.* **2002**, *14*, 228-231. b) S. Seki, S. Tagawa, *Polymer J.* **2007**, *39*, 277-293. c) A. Saeki, S. Seki, T. Sunagawa, K. Usida, S. Tagawa, *Philos. Mag. B* **2006**, *86*, 1261-1276. d) A. Saeki, Y. Koizumi, T. Aida, S. Seki. *Acc. Chem. Res.* **2012**, 45, 1193–1202.

[3] a) A. Acharya, S. Seki, A. Saeki, Y. Koizumi, S. Tagawa, *Chem. Phys. Lett.*, **2005**, *404*, 356-360. b) S. Seki, Y. Koizumi, T. Kawaguchi, H. Habara, S. Tagawa, *J. Am. Chem. Soc.* **2004**, *126*, 3521-3528.

[4] a) W. E. Ford, H. Hiratsuka, and Prashant V. Kamat. *J. Phys. Chem*. **1989**, *93*, 6692-6696. b) Aaron S. Lukas and Michael R. Wasielewski. *J. Phys. Chem. A*. **2000**, *104*, 6545-6551.